Implementation of a Deep Learning ANN-based Algorithm utilizing the IEEE 34 Bus Test System to Investigate the Effects of Distributed Generation on Fault Diagnosis in Distribution Networks

Parach Daniel Deng
Department of Electrical Engineering, Pan African University Institute for Basic Sciences, Technology and Innovation, Nairobi, Kenya
parachdan@gmail.com (corresponding author)

George K. Irungu
Department of Electrical Engineering, Jomo Kenyatta University of Agriculture and Technology, Nairobi, Kenya
girungu@jkuat.ac.ke

Josiah Munda
Department of Electrical Engineering, Tshwane University of Technology, Pretoria, South Africa
mundajl@tut.ac.za

Received: 1 October 2024 | Revised: 08 November 2024 | Accepted: 20 November 2024

 DOI: https://doi.org/10.48084/etasr.9153

ABSTRACT

Electrical distribution systems are undergoing significant modifications since the application of new technologies. New possibilities for automated, dependable, and efficient electrical power grids have been made possible by the technological advancement. While new technologies might improve electrical network performance and offer creative solutions to future network difficulties, they can also have unintended consequences that need to be carefully studied and considered. A recent technological advancement that enhances power grid performance is Distributed Generation (DG). While DG unit integration has measurable benefits for electrical grids, its significant effects on power network protection systems create many questions and difficulties about the proper way to identify and isolate distribution network faults. The DLANN-based approach looks into the ways the integration of DGs affects fault identification and location. This method involves two steps: first, three-phase currents are constantly analyzed for detection, and Discrete Wavelet Transform (DWT) is utilized to extract the currents' features. The second step is classification employing Artificial Neural Networks (ANNs) to pinpoint the defective stages. Counting the shorted phases will reveal the sort of short circuit. The MATLAB programming environment is utilized in the development of the fault identification and classification technique. The fault type (one, two, or three phases), fault resistance, fault location bus, fault distance, and the DG type (upstream or downstream) are all considered. The methodology is used on a modified IEEE 34-bus test system, and four scenarios, one with combined DGs units, one with IBDGs, one with SBDGs, and one without DGs, are modeled. As per the simulation results, 100% fault detection and classification accuracy were obtained, whereas the average fault location accuracy attained without DGs, with IBDGs, SBDGs and combined DGs for selected nodes were 99.94%, 99.91%, 99.86%, and 99.88%, respectively.

Keywords-distribution network; DLANN; fault detection; fault classification; fault location

I. INTRODUCTION

Power distribution systems are becoming more vulnerable to failures as a result of infrastructure problems like age and poor maintenance, which can cause insulation breakdowns that compromise the continuity and dependability of the power supply, as well as environmental factors like lightning or trees falling onto power lines [1]. The protection system's main responsibility is to rapidly identify defects, isolate the problematic feeder, and then precisely locate the fault. Precise fault localization lowers maintenance time, shortens service outages, and improves reliability metrics. However, due to the high energy demands, new developments in power electronics have made the application of DG more practical. This has altered the fault current's amplitude and direction, which affects how precisely standard protection systems locate faults. The main substation's measured currents and voltages are used to calculate the impedance in traditional fault location techniques, sometimes referred to as the distance-based method. These approaches are prone to large errors in distribution networks with DG units.

Conventional fault diagnostic techniques can be divided into knowledge-based methods, high-frequency component and traveling-wave-based techniques, and impedance and other basic frequency-based approaches [2]. Nevertheless, traveling-wave-based techniques have intrinsic drawbacks that require complicated structures, high sampling rates, wide-bandwidth high-speed communication links, and quick data synchronization [3, 4]. By contrast, impedance-based techniques show up as a simpler option to put into practice [5, 6]. However, if there are laterals in the network, impedance-based approaches necessitate intricate iterations and result in multiple estimations. In order to tackle this problem, a technique utilizing data from smart meters was suggested in [7, 8]. However, measurement inaccuracies, load variations, and the unpredictability of defect information reduced the method's accuracy [9]. Intelligent devices have allowed distribution utilities to acquire more data for fault analysis, and knowledge-based approaches can use these data to diagnose faults. In fault diagnosis, knowledge-based approaches have become more popular because of their generalizability and promising performance [10, 11]. ANNs, Fuzzy Logic Systems (FLSs), Decision Trees (DTs), Support Vector Machines (SVMs), and k-Nearest Neighbors (kNNs) are popular Machine Learning (ML) methods for fault location [1].

The term "deep" in Deep Learning (DL) is used to contrast it with additional layers of non-linear functions found in classic ML algorithms like SVM, ANN, and other not-deep learning techniques. Conventional ANN learning techniques require the manual extraction of data sample attributes. By using back-propagation to execute layer-by-layer feature transformation on the original data, DL, on the other hand, automatically learns to produce feature representations. These hierarchical feature representations are very abstract and task-oriented. One of the main advantages of DL is that it can learn from raw data to the outcomes of classification and regression tasks in an end-to-end manner. Deep Belief Networks (DBNs) [12], autoencoder (AE) [13], Convolutional Neural Network (CNNs) [14], and Recurrent Neural Networks (RNNs) [15] are examples of common DL designs. The problems of intelligent industrial defect diagnosis in distribution networks have seen the introduction of numerous innovative architectures due to the rapid development of DL techniques. Transformer [17], Generative Adversarial Network (GAN) [16], and Graph Neural Network (GNN) [18] are a few examples. In the field of optical flaw detection, the DL approach using CNN has proven to be incredibly effective, particularly when used to large PV plants [19]. UAV-collected image data are typically used [20]. DL methods have demonstrated encouraging outcomes in terms of fault detection accuracy and speed. On the other hand, the requirement for big datasets, specialized gear, and knowledgeable staff limits DL's immediate real-time feasibility. By employing DL for fault identification, IBDG algorithms are able to recognize and categorize particular abnormalities according to the features of the provided dataset [21]. Additionally, the learning parameters of a given algorithm can be changed for the specific defect detection. When analysis is needed in a short amount of time, a small dataset or sample size problem occurs [22]. It can occasionally have a detrimental effect on the detection method, but creating a sizable dataset can be difficult. Because noise and outliers affect DL's feature learning capabilities, data pre-processing is also a difficult task [23]. Furthermore, altering the DL architecture to increase accuracy is a challenging process that calls for expertise and domain knowledge. Three approaches, data pre-processing, feature extraction and selection, and classification are often used as steps in a DL-based defect detection and classification process. The availability of computational resources and needs determines the utilized strategy [24]. One strategy is the use of DL-based classification models, statistical analysis models for pre-processing and feature extraction, and signal analysis [25]. By using this method, classification accuracy is improved and complexity is decreased. Another strategy is the adaption of traditional statistical analysis methods for pre-processing and using DL models for feature selection and classification. Because categorization is based on unsupervised extracted features, this method eliminates the need for user involvement. A third strategy is an end-to-end method that computes output straight from the input, involves using DL models to classify raw data [26]. The contributions of this paper include:

- A Deep Learning Artificial Neural Network (DLANN)-based algorithm for fault detection, classification and location in a distribution network is developed.
- DLANN and Discrete Wavelet Transformation (DWT) were developed for the localization, classification, and detection of faults.

II. MATERIALS AND METHODS

In this section, the proposed DLANN-based algorithm is designed and trained. The process involves designing the fault diagnosis distribution line model block, modelling of IEEE 34 Bus system without and with DGs and finally conducting simulations in MATLAB environment.

A. Design of the Fault Diagnosis Block Model of the Proposed System

The modeling of a distribution network consists of lines, transformers, and other components as shown in Figure 1. A

MATLAB model that was simulated to produce fault signals was created using the model and the real system parameters of the IEEE 34 bus system. The MATLAB/SIMULINK environment was used to construct the distribution line. Sections considered on the line were of several kms, with 11 kV and 50 Hz power line on the IEEE 34 bus test system. The system analyzed postfault conditions and all the conducted simulations generated fault signals which were used to identify and locate the faults and generate a database. Faults were created at every section of the IEEE 34 bus radial feeder line (buses) and a bigger data base was created and used in the development and designing of the DLANN system which is reliable and accurate in distance estimation and fault classification. Figure 2 shows the proposed framework for fault diagnosis with IBDGs and SBDGs whereas the flowchart for the proposed algorithm is shown in Figure 3.

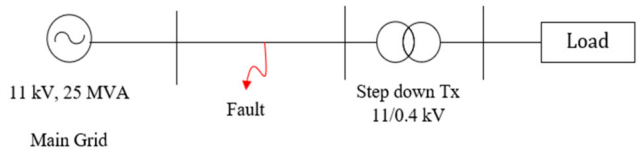

Fig. 1. A 11 kV three-phase, 10 km distribution line model.

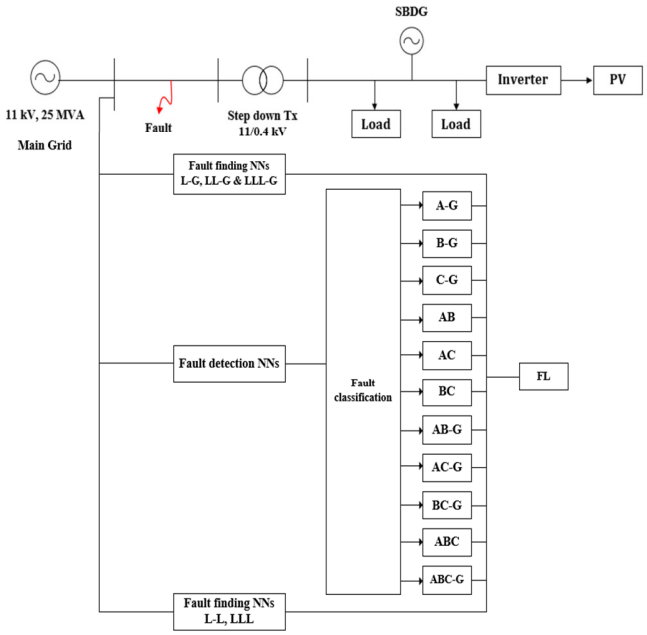

Fig. 2. Proposed framework for fault diagnosis with IBDGs and SBDGs.

B. The DLANN Model for Fault Diagnosis

ANNs consist a key ML tool that has experienced exponential growth in the past 10 years. Their remarkable ability to identify patterns in data that are far too complex for simple linear systems to recognize has fueled their use. Essentially, utilizing examples that generate input–output mappings based on a model equation developed from the iterative training process, ANNs learn to recognize complicated patterns in data. Through training, an ANN learns to identify patterns in the data and generates a generalized model equation using the historical data that is fed into the network. This research offers models combining multi-layer feedforward neural networks, commonly known as Multi-Layer Perceptrons (MLPs), and sigmoid activation functions for backward propagation-based defect location identification, fault detection, and classification. In this kind of ANNs, there are three primary layers: the input layer, the output layer, and the hidden layer(s). The input layer is the initial layer in a neural network, as seen in Figure 4. It transfers values, or input signals, to the following layer. The input signals (values) are not subjected to any procedures, and there are no weights or biases applied. Eight input signals, namely three phase voltages (x_1, x_2, x_3), three phase currents (x_4, x_5, x_6), zero sequence voltage (x_7), and zero sequence current (x_8) are represented in this network.

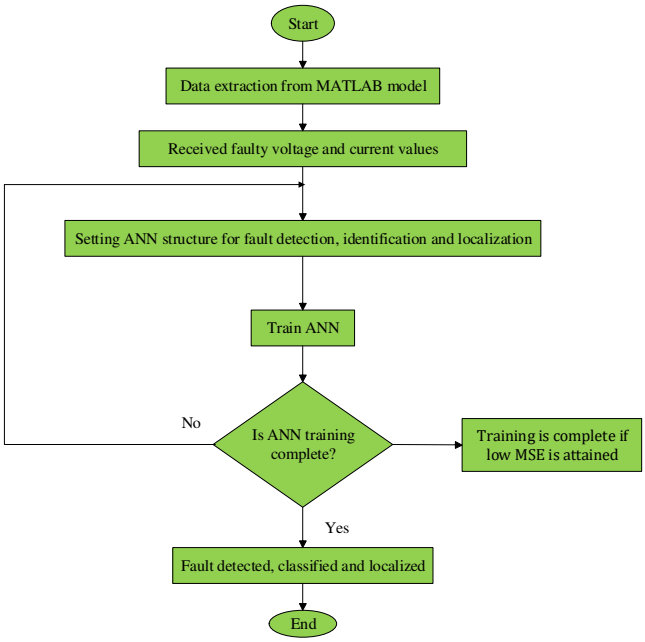

Fig. 3. Flowchart of the proposed algorithm.

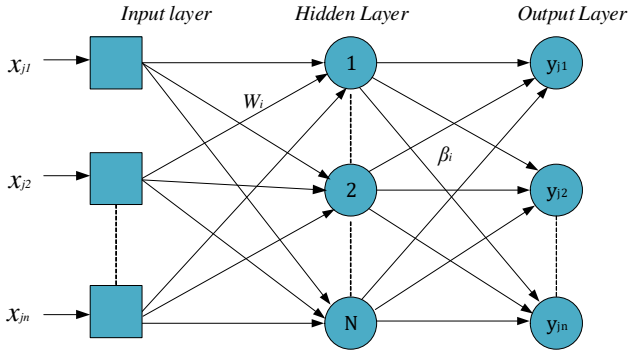

Fig. 4. Model of the neural network.

Five outputs from the ANN are utilized to locate and classify faults. Three phases and one ground are used for classification, and the final output gives information on the fault's location on the distribution line. Figure 4 displays the

developed ANN model. The final layer in the network, known as the output layer, gets data from the final hidden layer. This layer allows one to obtain the necessary range and quantity of values. The output layer of this network has 10 neurons that produce the outputs y_1, y_2, y_3, y_4, and y_5. The network designer has added hidden neurons to the hidden layer(s) to link the input and output layers. Neurons, or nodes, in hidden layers perform various modifications on the input data.

C. Simulations of the Proposed System

The Simulink model for fault detection, classification, and location in Figure 5 was opened following a successful training session, enabling the detection, classification, and localization of faults.

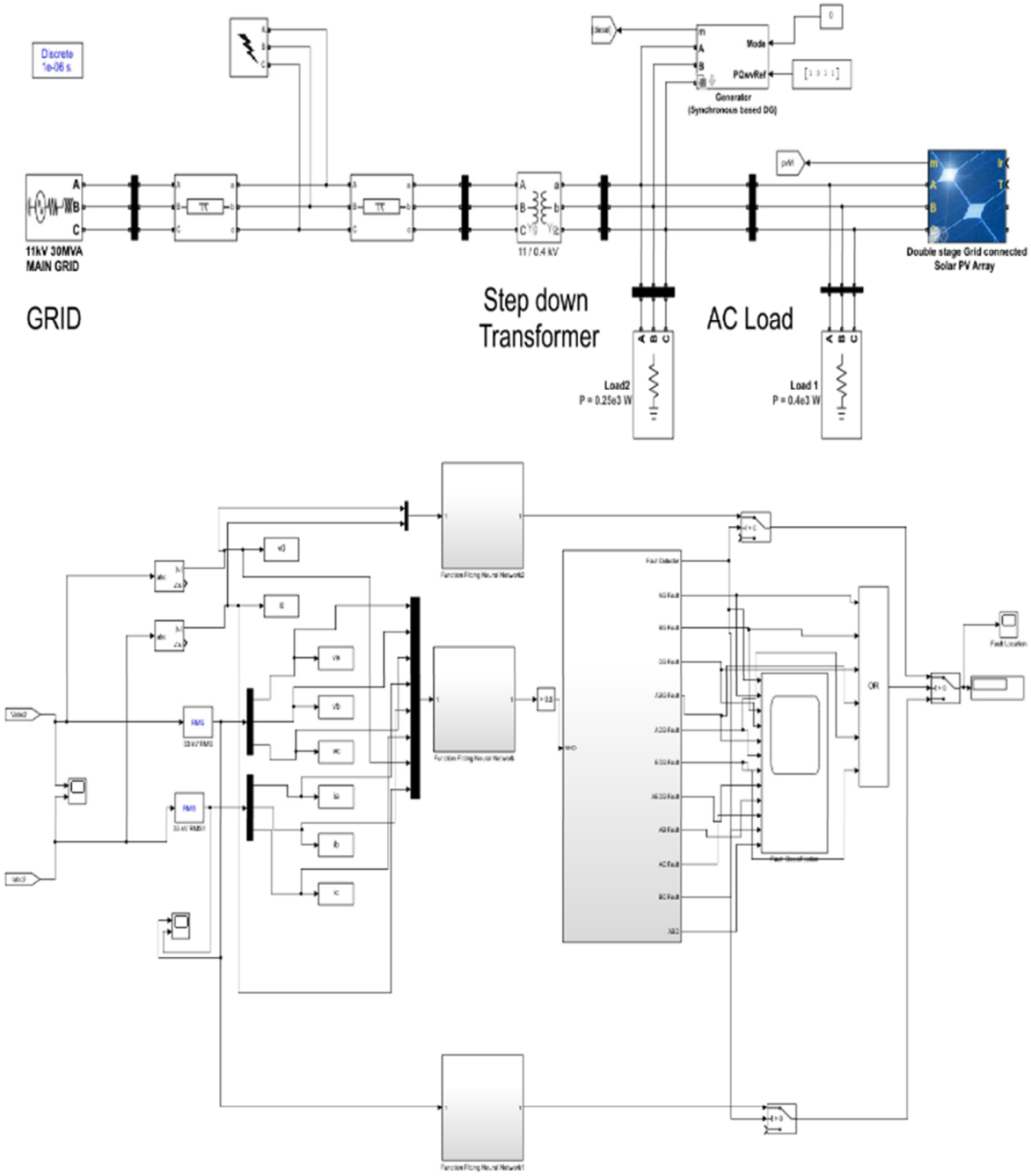

Fig. 5. Simulink models for diagnosis with DGs.

1) Steps

- Choose Phase *A*, phase *B*, phase *C*, and ground at a time from the three phase multi-fault block and mark e.g. *AG*, *AB, BCG, ABC*, etc.
- Choose fault occurrence time and clearing time in switching from 0.1 to 0.2 s in the model
- Δifferent fault resistance values were considered, from 0.1 to 1 Ω.
- Simulate the Simulink model and open the various scopes.
- A fault occurs at 0.1 s, changing the output from 0 to 1. A system fault is represented by a 1 whereas a 0 indicates no fault.
- The fault detector is set from 0 to 1 in order to indicate faults.
- The remaining findings are kept at 0 for no fault classification, and the *AG* fault is changed from 0 to 1.
- The fault location is recorded in the display for each type fault detected and classified.

2) Simulink Model Description

- The model consists of three buses, two source buses and one load bus.
- The distribution line length is 10 km with a pi-model and a 11/0.4 kV step-down transformer.
- A three-phase fault is created along the distribution line and some codes are used to execute line fault model.
- After running the codes, some input and output data are generated and used to train the ANN.

3) Neural Network Block Description

Three ANNs were employed, one for finding fault detection, another for finding phase to ground faults, and a third for finding phase to phase faults. The neural network for detecting faults receives 8 inputs of voltages and currents along with its zero sequence values i.e. *Va, V_b, Vc, Ia, I_b, I_c, V_o*, and I_o and its output is in logic form and is thus encoded to classify the faults by using classification block. The fault finding ANN block of phase to ground faults, receives 2 inputs, i.e. zero sequence voltage *Vo* and current *Io* and its output is fault location. The fault finding ANN for line-to-line faults has as only input the rms voltage and fault location is its output.

III. RESULTS AND DISCUSSION

The developed DLANN model was implemented in 6-bus fault locations on IEEE 34-bus network and is discussed below.

A. Modeling of the IEEE 34 Bus Test System

The IEEE-34 bus test system is utilized in the simulations of many problem scenarios. It is made up of a large, lightly loaded real feeder in North America with a nominal voltage of 24.9 kV and 12 MVA. The source feeder was scaled down to 11 kV. Single-phase and three-phase loads, as well as single- and double-phase side branches, are present in its main feeder. The primary features of the IEEE-34 bus are as: A balanced concentrated load and an unbalanced distributed load, two voltage regulators, an in-line transformer to reduce voltage from 24.9 kV to 11 kV, and shunt capacitors [27]. Variations in the impedance and voltage drop along the distribution lines are introduced by the model's various feeders of varying lengths. This reflects the intrinsic properties of distribution networks, where different line lengths can result in different voltage drops and line losses. Due to the feeder lengths and variability in load and feeder characteristics, the IEEE 34 bus model is especially well-suited for modelling the integration of DG systems, including synchronous and inverter-based DGs. Its small size allows it to be computationally economical while retaining enough complexity to represent the dynamics of a distribution system. Its scalability allows for the examination of the effects of DG integration without putting an undue strain on computing.

A MATLAB model was created for the modified IEEE-34 bus. A constant impedance model is used to model the loads, and all fault combinations are simulated [28]. Algorithms for short-circuit location, classification, and detection were created in the MATLAB® environment. Every simulation was run on a PC equipped with a 2.90–2.92 GHz Intel Core i7 processor and 16 GB of RAM. The IEEE-34 bus system was used to represent four distinct scenarios in order to assess the suggested methodology. Variations in the following characteristics are considered while performing different short-circuit conditions: fault resistance, short-circuit type, fault location bus, and DG units.

As seen in Figure 6(a), the IEEE-34 bus test system is modeled in the first scenario without DG units. In Figure 6(b) in the second case, only synchronous based DGs (DG_1, DG_2, DG_3, DG_4 and DG_5) were considered and inserted at the candidate buses 808, 816, 854, 848 and 840, respectively. The interface nominal voltages for the SBDGs connection are 220 V for DG_2 and DG_5 and 480 V for DG_1, DG_3, and DG_4. Figure 6(c) shows the third scenario, where only IBDGs are connected to the same buses as above. The total PV model applied in this study is 1 MVA of installed power. Each IBDG has a capacity of 0.2 MVA. Figure 6(d) shows the case with combined DGs. The fault location points are F802, F806, F808, F824, F856, and F840. The primary feeder is 115.35 km long and runs between nodes 800 and 840. Due to the length of this feeder, it becomes more challenging to locate faults using information that can only be found at the substation.

B. Simulink Parameters

The key Simulink parameters used in this work include fault resistance, DG location specifics, and DG integration interface. The criteria for determining these parameters and how they influence fault diagnosis in distribution network are discussed below.

1) Fault Resistance

A number of tests were carried out to assess the accuracy of the suggested system under the fluctuation of fault resistance. For each IEEE 34 radial line section in the network, the average fault location errors for 11 different types of failures that were simulated at the sending, middle, and receiving

locations were shown. It was assumed that the fault resistances were 0.01, 0.1, and 1 Ω. The findings in this section demonstrate that the fault localization error is relatively small for 0.01 fault resistance scenarios and increases with increasing fault resistance.

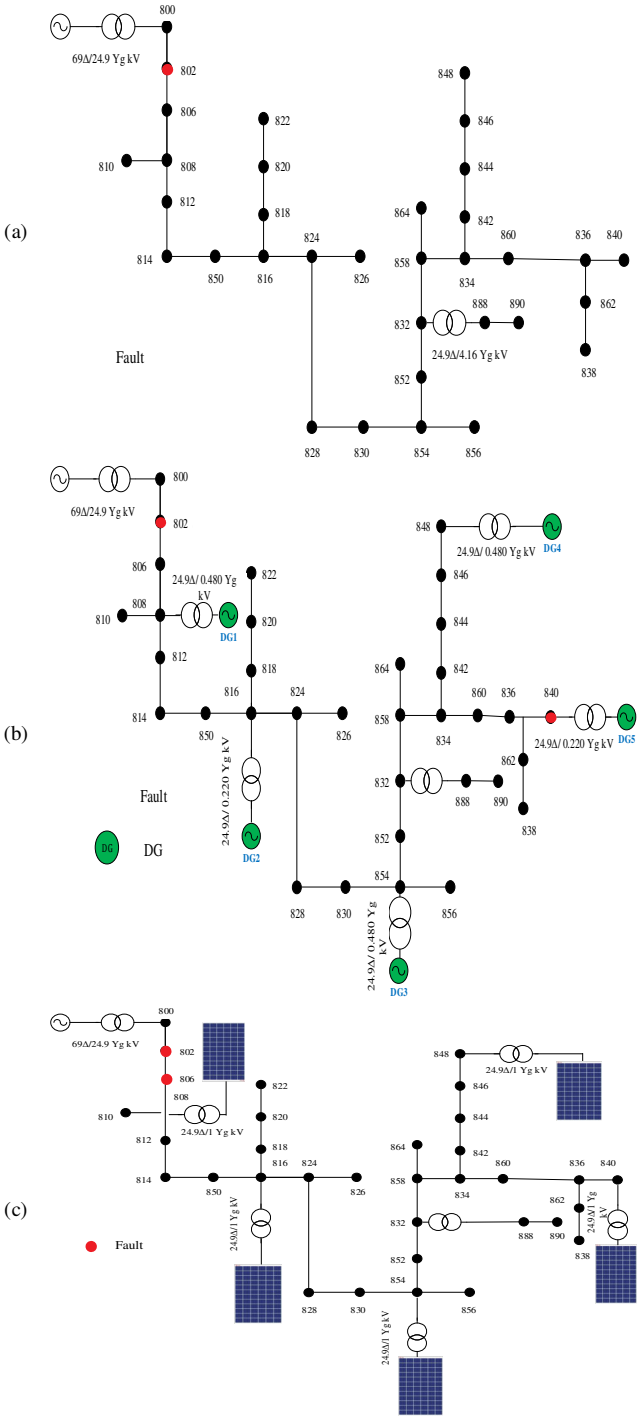

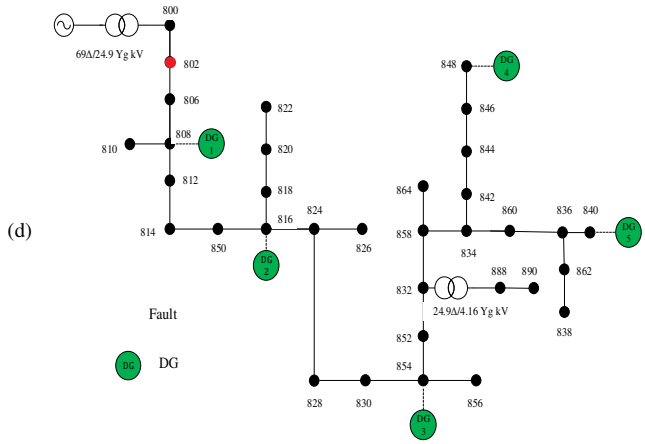

Fig. 6. IEEE-34 bus test system fault simulation: (a) without DG units, (b) with SBDGs, (c) with IBDGs, (d) with both IBDGs and SBDGs.

2) DG Location Specifics

To determine the ideal size and location of DG units, a load flow analysis of the IEEE 34 bus test system was conducted using the Newton Raphson method [29]. As seen in Figure 6, the candidate buses with DGs installed are 808, 816, 854, 848, and 840. Two factors were used to establish the DG location: at first, the voltage fluctuation at the buses was taken into consideration, and DGs were installed at weak buses to improve the voltage profile. Second, in order to minimize losses, DGs were installed at buses with larger line losses.

3) DG Integration

Fault location accuracy in a distribution network is lower when DG units are integrated than when they are absent because of the critical challenges introduced by the integration of DGs [30] such as dynamics and variances in the amplitude of fault current and loss of relay sensitivity and protection blindness, given that microgrids can function in both isolated and grid-connected modes. Fault diagnosis accuracy depends on the type of DG connected. The considered types in this study were IBDGs and SBDGs. The fault current contribution is influenced by the type of DG units. Inverter-interfaced DG units can contribute up to 1.5 times their nominal current, whereas synchronous generators can produce fault currents approximately five times their normal current. An IBDG has better accuracy compared to SBDG because it injects less short circuit current. These difficulties lead to changes in the fault current magnitude (dynamics and variances), which complicates the process of locating and protecting the fault.

When a distributed generation unit is positioned in close proximity to the main substation, it may exacerbate a fault current in a parallel feeder. Relay mal-operation may come from the fault current contribution of the DG, which could produce false findings (loss of sensitivity). When a failure occurs at the end of the feeder that contains a DG unit, the feeder relay notices a lower fault current (protection blindness) because of the DG impedance. Reducing fault current magnitudes results in an underestimation of fault current and may prevent the relay from isolating the problem. This underestimation could impede the protection system response

and the subsequent identification of the malfunction. Furthermore, if overlooked, it could have an impact on the estimation's accuracy. Numerous buses along the feeder were considered for 11 different kinds of simulated short circuits. Table I presents the system parameters used for the various fault scenarios. Consideration is given to short circuits with varying resistance values.

TABLE I. IEEE-34 BUS TEST SYSTEM PARAMETERS FOR FAULT SIMULATIONS

Parameters	Configurations
Fault types	A-G, B-G, CG, AB-G, AC-G, BC-G, ABC-G, AB, AC, BC, ABC
Fault location bus	802, 806, 808, 824, 856, 840
DG units	IBDGs and SBDGs
Fault resistance	0.01 Ω and greater than 1 Ω (LIF)

C. Fault Diagnosis at a Constant Low Fault Resistance

In this section, cases without DGs, with IBDGs, SBDGs and both IBDGs and SBDGs were considered in separate simulations and the DLANN was evaluated by applying cases with impedance faults on the IEEE 34 bus radial feeder in several lengths from the substation. The fault was simulated in several nodes of the IEEE 34 radial feeder i.e. 802 (1.573 km), 806 (2.625 km), 808 (22.275 km), 824 (69.676 km), 856 (97.19 km), and 840 (115.35 km) away from the source grid. The achieved fault detection and classification accuracy were 100% whereas the average fault location accuracy for the case without DGs, with IBDGs or SBDGs, and both DGs at this impedance value for the above nodes on the IEEE 34 bus radial feeder was about 99.94%, 99.91%, 99.88%, and 99.86% respectively. Therefore, all the fault types were accurately detected, classified, and located for 0.01 Ω fault resistance. The simulation results for the fault detection, classification and location on 11 sections on the distribution network are exhibited in Tables II-V and Figures 7-10. It is easy to observe that the location system provided good results.

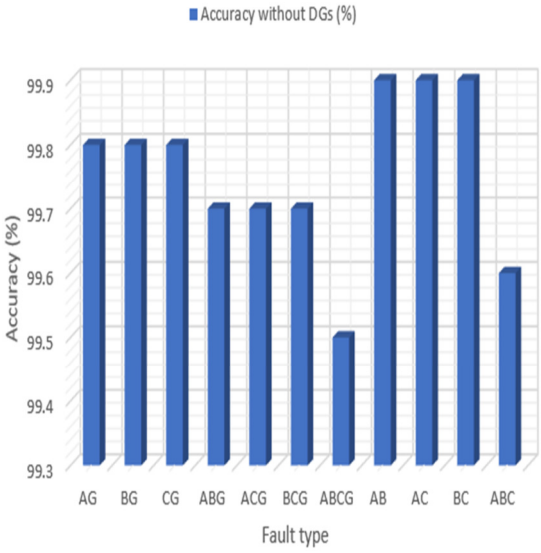

Fig. 7. Fault location accuracy without DGs at node 806 (2.625 km) for different fault types.

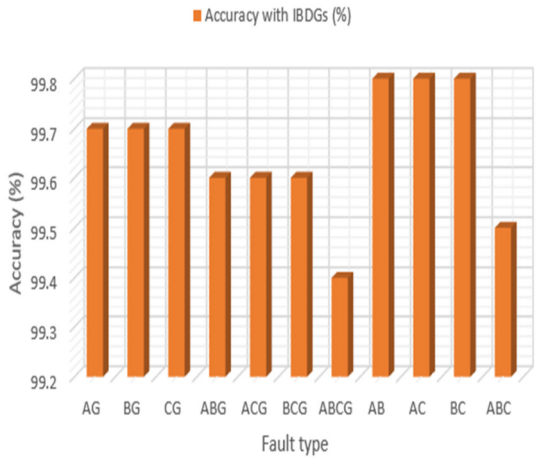

Fig. 8. Fault location accuracy with IBDGs at node 806 (2.625 km) for different fault types.

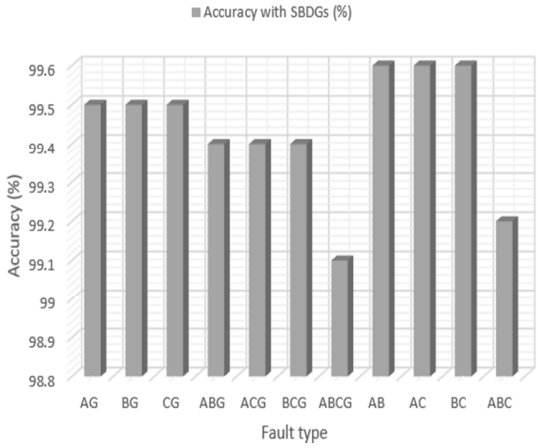

Fig. 9. Fault location accuracy with SBDGs at node 806 (2.625 km) for different fault types.

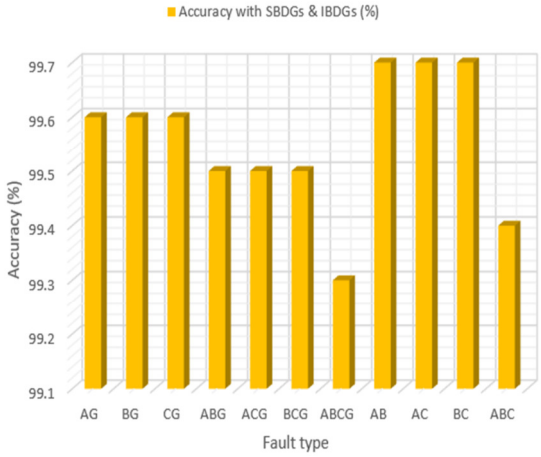

Fig. 10. Fault location accuracy with IBDGs and SBDGs at node 806 (2.625 km) for different fault types.

TABLE II. FAULT DETECTION, CLASSIFICATION, AND LOCATION FOR SHORT CIRCUITS ON THE IEEE-34 BUS FEEDER AT NODE 806 WITHOUT DGS

Fault type	R_f (Ω)	Fault detection	Fault classification	Node 806 (2.625 km)	Estimated fault location (km)	Relative error (%)	Accuracy (%)
AG	0.01	√	√	2.625	2.815	0.2	99.8
BG	0.01	√	√	2.625	2.714	0.2	99.8
CG	0.01	√	√	2.625	2.687	0.2	99.8
ABG	0.01	√	√	2.625	2.954	0.3	99.7
ACG	0.01	√	√	2.625	2.941	0.3	99.7
BCG	0.01	√	√	2.625	2.961	0.3	99.7
ABCG	0.01	√	√	2.625	2.113	0.5	99.5
AB	0.01	√	√	2.625	2.549	0.1	99.9
AC	0.01	√	√	2.625	2.684	0.1	99.9
BC	0.01	√	√	2.625	2.543	0.1	99.9
ABC	0.01	√	√	2.625	2.159	0.4	99.6

TABLE III. FAULT DETECTION, CLASSIFICATION, AND LOCATION FOR SHORT CIRCUITS ON THE IEEE-34 BUS FEEDER AT NODE 806 WITH IBDGS

Fault type	R_f (Ω)	Fault detection	Fault classification	Node 806 (2.625 km)	Estimated fault location (km)	Relative error (%)	Accuracy (%)
AG	0.01	√	√	2.625	2.151	0.45	99.5
BG	0.01	√	√	2.625	2.138	0.46	99.5
CG	0.01	√	√	2.625	2.122	0.47	99.5
ABG	0.01	√	√	2.625	1.970	0.57	99.4
ACG	0.01	√	√	2.625	1.890	0.64	99.4
BCG	0.01	√	√	2.625	1.940	0.59	99.4
ABCG	0.01	√	√	2.625	1.619	0.87	99.1
AB	0.01	√	√	2.625	2.135	0.43	99.6
AC	0.01	√	√	2.625	2.145	0.42	99.6
BC	0.01	√	√	2.625	2.153	0.41	99.6
ABC	0.01	√	√	2.625	1.731	0.80	99.2

TABLE IV. FAULT DETECTION, CLASSIFICATION, AND LOCATION FOR SHORT CIRCUITS ON THE IEEE-34 BUS FEEDER AT NODE 806 WITH SBDGS

Fault type	R_f (Ω)	Fault detection	Fault classification	Node 806 (2.625 km)	Estimated fault location (km)	Relative error (%)	Accuracy (%)
AG	0.01	√	√	2.625	2.151	0.45	99.5
BG	0.01	√	√	2.625	2.138	0.46	99.5
CG	0.01	√	√	2.625	2.122	0.47	99.5
ABG	0.01	√	√	2.625	1.970	0.57	99.4
ACG	0.01	√	√	2.625	1.890	0.64	99.4
BCG	0.01	√	√	2.625	1.940	0.59	99.4
ABCG	0.01	√	√	2.625	1.619	0.87	99.1
AB	0.01	√	√	2.625	2.135	0.43	99.6
AC	0.01	√	√	2.625	2.145	0.42	99.6
BC	0.01	√	√	2.625	2.153	0.41	99.6
ABC	0.01	√	√	2.625	1.731	0.80	99.2

TABLE V. FAULT DETECTION, CLASSIFICATION, AND LOCATION FOR SHORT CIRCUITS ON THE IEEE-34 BUS FEEDER AT NODE 806 WITH IBDGS AND SBDGS

Fault type	R_f (Ω)	Fault detection	Fault classification	Node 806 (2.625 km)	Estimated fault location (km)	Relative error (%)	Accuracy (%)
AG	0.01	√	√	2.625	2.135	0.43	99.6
BG	0.01	√	√	2.625	2.145	0.42	99.6
CG	0.01	√	√	2.625	2.153	0.41	99.6
ABG	0.01	√	√	2.625	2.151	0.45	99.5
ACG	0.01	√	√	2.625	2.138	0.46	99.5
BCG	0.01	√	√	2.625	2.122	0.47	99.5
ABCG	0.01	√	√	2.625	1.789	0.73	99.3
AB	0.01	√	√	2.625	2.310	0.27	99.7
AC	0.01	√	√	2.625	2.319	0.27	99.7
BC	0.01	√	√	2.625	2.346	0.24	99.7
ABC	0.01	√	√	2.625	2.101	0.55	99.4

D. Effect of Fault Distance on Fault Diagnosis Results for Fault Resistance 0.01 Ω.

Simulations were conducted on the IEEE 34 bus system without and with IBDGs, SBDGs, and both. The obtained results aew recorded in Table VI and the comparisons of the average fault location accuracy is shown in Figure 11. The analysis of the results shows that, average fault location accuracy was 99.53%, 99.38%, 99.25%, and 99.32% when considering no DGs, IBDGs, SBDGs, and both IBDGs and SBDGs. Fault location accuracy was the highest (99.53%) for the case without DGs because there is no DGs influence or contribution of DG fault current level to the distribution network that could affect the fault location accuracy. The second fault location accuracy was obtained for the case with IBDGs (99.38%) because the IBDGs do not tolerate high levels of fault current due to the presence of power electronic devices. The average fault location accuracy of the combined IBDGs and SBDGs was 99.32% which was midway between IBDGs and SBDGs. The overall results showed that the fault location accuracy without DGs (99.53%) is better than when utilizing DGs whether being IBDGs or SBDGs, because when DGs are added to the distribution network, the DGs influence the fault current level, something that reduces fault location accuracy.

TABLE VI. AVERAGE FAULT LOCATION SIMULATION RESULT COMPARISON FOR SHORT CIRCUITS ON IEEE-34 BUS NODES FOR $R_f = 0.01\ \Omega$

Node/Actual fault distance (km)	Average fault location accuracy without DGs (%)	Average fault location accuracy with IBDGs (%)	Average fault location accuracy with SBDGs (%)	Average fault location accuracy with both DG types (%)
802 (1.573)	99.93	99.92	99.87	99.90
806 (2.625)	99.84	99.70	99.64	99.66
808 (22.275)	99.73	99.57	99.39	99.41
824 (69.676)	99.59	99.38	99.28	99.35
856 (97.190)	99.27	99.25	99.18	99.23
840 (115.35)	98.83	98.43	98.13	98.36

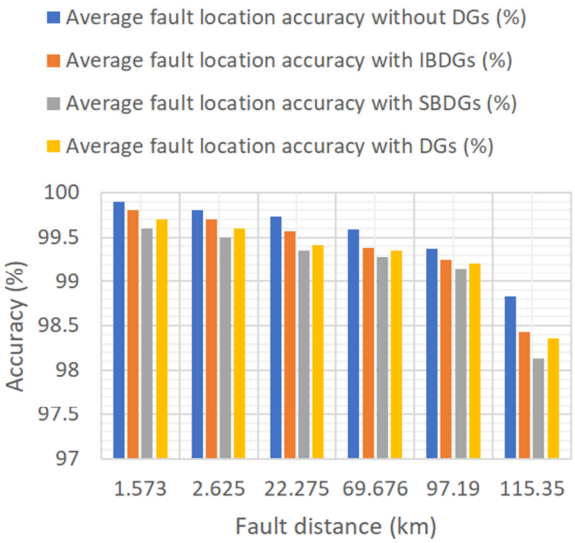

Fig. 11. Comparison of average fault location accuracy versus fault distance without and DG units.

For the same fault types, e.g. LG, LLG, LLLG, LL, and LLL, the fault location accuracy varies. From Figure 12 and Table VII, it can be observed that the case without DGs has the highest accuracy, followed by IBDGs, both DGS, and SBDGs. The Figure shows differences in the shape of the fault pattern due to differences in the DG consideration. Also, each fault type has different values of fault resistances, although fault resistance was assumed to be the same for all the types of faults, the phase to phase (AB, AC and BC) faults have lower resistance and higher accuracy compared to three phase faults (ABCG).

The accuracy of the fault location is influenced by the fault location distance. Faults that occurred close to the substation have better accuracy compared to those that are away from the substation, because near the substation (where the measurement points are located), the fault current increases and the impedance of the fault decreases and so the fault can be detected and located easily (accurately). As one moves away from the substation, the fault current decreases and the fault resistance increases. Fault location errors are presented in Table VIII and Figure 13. It can be observed that, fault location accuracy without DGs has the lowest error, followed by IBDGs, both DGs, and SBDGs.

TABLE VII. FAULT LOCATION ACCURACY ON IEEE-34 BUS FEEDER AT NODE 806 WITH AND WITHOUT DGs

Fault type	R_f (Ω)	Node 806 (2.625 km)	Accuracy (%)			
			Without DGs	With IBDGs	With SBDGs	With both DGs
LG	0.01	2.625	99.8	99.7	99.5	99.6
LLG	0.01	2.625	99.7	99.6	99.4	99.5
LLLG	0.01	2.625	99.5	99.4	99.1	99.3
LL	0.01	2.625	99.9	99.8	99.6	99.7
LLL	0.01	2.625	99.6	99.5	99.2	99.4

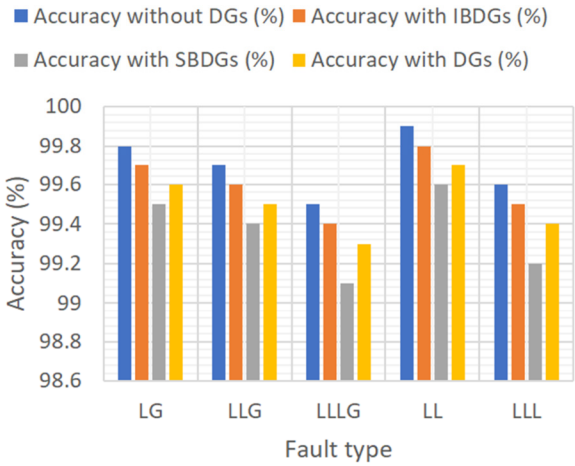

Fig. 12. Comparison of fault location accuracy versus fault types with and without DGs.

TABLE VIII. FAULT LOCATION ERRORS WITH AND WITHOUT DGs

Node/Actual fault distance (km)	Fault location error (%)			
	Without DGs	With IBDGs	With SBDGs	With IBDGs and SBDGs
1.573	0.07	0.08	0.13	0.10
2.625	0.16	0.30	0.36	0.34
22.275	0.27	0.43	0.61	0.59
69.676	0.41	0.62	0.72	0.65
97.190	0.73	0.75	0.82	0.77
115.350	1.17	1.57	1.87	1.64

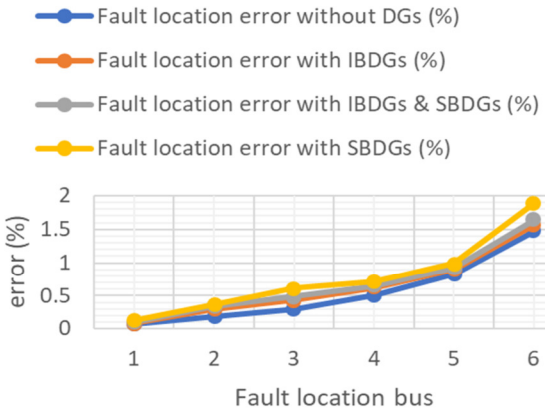

Fig. 13. Fault location error with and without DGs.

E. Effect of Fault Distance on IEEE 34 Bus Fault Diagnosis Results for Fault Resistance of 0.01 Ω

In the above, fault diagnosis was conducted for the case of one terminal measurement, whereas in this section, simulation for two end terminal measurement is carried out and the results obtained for the IEEE 34 bus feeder at node 806 without and with DGs are plotted and recorded Figures 14-17 and Tables IX-X.

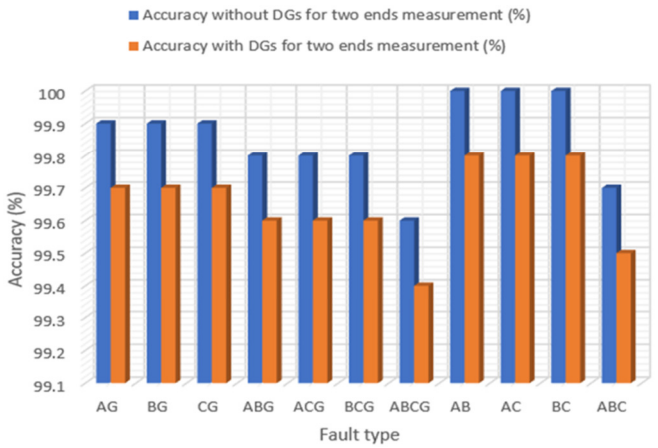

Fig. 14. Fault diagnosis on IEEE 34 bus at node 806 for two end measurement with and without DGs.

A comparison was also made for the two cases of measurement. The comparative results for two terminal measurement swith and without DGs are shown in Table XI, whereas the comparative results for one and two end terminal measurement are shown in Table XII. The two end terminal measurement gives more accurate results compared to one end terminal measurement because there are many measurement points both from the substation (beginning of the line) and at the end of the distribution line. Therefore, the fault signals will be detected more easily. The method of two end terminal measurement can be enforced by installing synchronous Phasor Measurement Units (PMUs) at both ends of the line and this helps in reducing the fault location errors compared to one end terminal measurement.

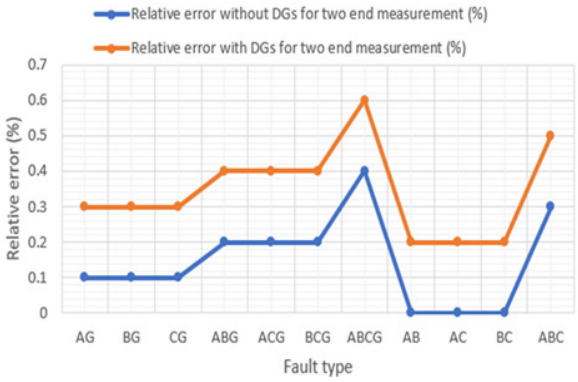

Fig. 15. Comparison of relative error with and without DGs for two end measurement.

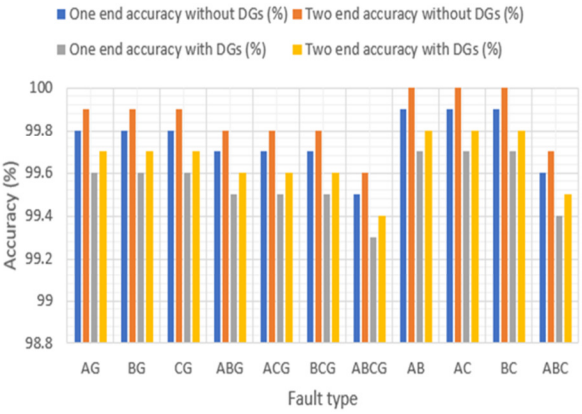

Fig. 16. Accuracy comparison of fault diagnosis results for one and two end measurement accuracy with and without DGs on the IEEE 34 bus system at node 806.

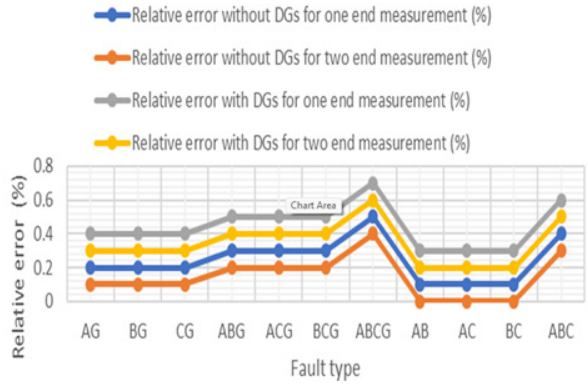

Fig. 17. Relative error comparison with and without DGs for one and two end measurement.

TABLE IX. FAULT DETECTION, CLASSIFICATION, AND LOCATION FOR SHORT CIRCUITS ON THE IEEE-34 BUS FEEDER AT NODE 806 WITHOUT DGs FOR TWO END MEASUREMENT

Fault type	R_f (Ω)	Fault detection	Fault classification	Node 806 (2.625 km)	Estimated fault location (km)	Relative error (%)	Accuracy (%)
AG	0.01	√	√	2.625	2.720	0.1	99.9
BG	0.01	√	√	2.625	2.680	0.1	99.9
CG	0.01	√	√	2.625	2.563	0.1	99.9
ABG	0.01	√	√	2.625	2.831	0.2	99.8
ACG	0.01	√	√	2.625	2.850	0.2	99.8
BCG	0.01	√	√	2.625	2.795	0.2	99.8
ABCG	0.01	√	√	2.625	1.987	0.4	99.6
AB	0.01	√	√	2.625	2.631	0.0	100
AC	0.01	√	√	2.625	2.575	0.0	100
BC	0.01	√	√	2.625	2.602	0.0	100
ABC	0.01	√	√	2.625	2.230	0.3	99.7

TABLE X. FAULT DETECTION, CLASSIFICATION, AND LOCATION FOR SHORT CIRCUITS ON THE IEEE-34 BUS FEEDER AT NODE 806 WITH DGs FOR TWO END MEASUREMENT

Fault type	R_f (Ω)	Fault detection	Fault classification	Node 806 (2.625 km)	Estimated fault location (km)	Relative error (%)	Accuracy (%)
AG	0.01	√	√	2.625	2.29	0.3	99.7
BG	0.01	√	√	2.625	2.25	0.3	99.7
CG	0.01	√	√	2.625	2.31	0.3	99.7
ABG	0.01	√	√	2.625	2.20	0.4	99.6
ACG	0.01	√	√	2.625	2.15	0.4	99.6
BCG	0.01	√	√	2.625	2.14	0.4	99.6
ABCG	0.01	√	√	2.625	1.91	0.5	99.5
AB	0.01	√	√	2.625	2.43	0.2	99.8
AC	0.01	√	√	2.625	2.38	0.2	99.8
BC	0.01	√	√	2.625	2.44	0.2	99.8
ABC	0.01	√	√	2.625	2.00	0.5	99.5

TABLE XI. COMPARISON OF FAULT DIAGNOSIS RESULTS WITH AND WITHOUT DGs FOR TWO TERMINAL END MEASUREMENT USING DLANN

Fault type	Accuracy without DGs (%)	Accuracy with DGs (%)
AG	99.9	99.7
BG	99.9	99.7
CG	99.9	99.7
ABG	99.8	99.6
ACG	99.8	99.6
BCG	99.8	99.6
ABCG	99.6	99.4
AB	100	99.8
AC	100	99.8
BC	100	99.8
ABC	99.7	99.5

TABLE XII. COMPARISON OF ONE AND TWO END MEASUREMENT ACCURACY WITH AND WITHOUT DGs

Fault type	Accuracy without DGs (%)		Accuracy with DGs (%)	
	One end	Two end	One end	Two end
AG	99.8	99.9	99.6	99.7
BG	99.8	99.9	99.6	99.7
CG	99.8	99.9	99.6	99.7
ABG	99.7	99.8	99.5	99.6
ACG	99.7	99.8	99.5	99.6
BCG	99.7	99.8	99.5	99.6
ABCG	99.5	99.6	99.3	99.4
AB	99.9	100	99.7	99.8
AC	99.9	100	99.7	99.8
BC	99.9	100	99.7	99.8
ABC	99.6	99.7	99.4	99.5

F. Effect of Fault Resistance on IEEE 34 Bus Fault Diagnosis Results

This section looks into how fault resistance in the presence of DGs impacts fault location algorithms. Simulations were conducted without DGs, with IBDGs, with SBDGs and with both IBDGs and SBDGs at varying fault resistances. All the 11 types of fault were simulated on node 802 of the IEEE 34 bus radial distribution (at a distance of 1.573 km from the substation) and the results are shown in Tables XIII-XVI. Fault resistance varied from 0.1 to 1.0 Ω in intervals of 0.1 Ω. The results showed that fault location accuracy drops with the increase in fault resistance as shown in Figures 18-21.

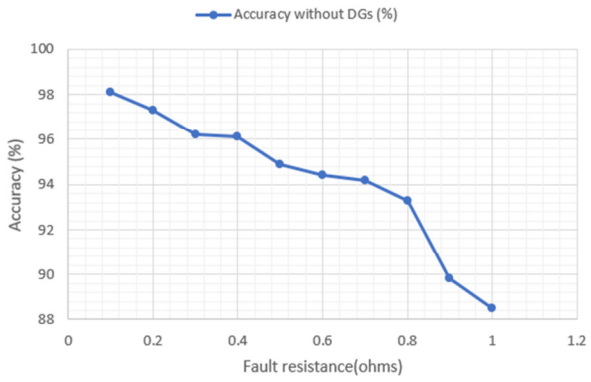

Fig. 18. Fault resistance versus accuracy for all fault types without DGs.

TABLE XIII. FAULT DETECTION, CLASSIFICATION, AND LOCATION ON IEEE-34 BUS FEEDER AT NODE 802 WITHOUT DGs

R_f (Ω)	Fault detection	Fault classification	Node 806 (1.625 km)	Estimated fault location (km)	Absolute error	Relative error (%)	Accuracy (%)
0.1	√	√	1.573	1.543	0.03	1.91	98.1
0.2	√	√	1.573	1.531	0.042	2.76	97.3
0.3	√	√	1.573	1.514	0.059	3.75	96.2
0.4	√	√	1.573	1.512	0.061	3.88	96.1
0.5	√	√	1.573	1.492	0.081	5.15	94.9
0.6	√	√	1.573	1.485	0.088	5.59	94.4
0.7	√	√	1.573	1.481	0.092	5.85	94.2
0.8	√	√	1.573	1.678	0.105	6.68	93.3
0.9	√	√	1.573	1.413	0.160	10.17	89.8
1.0	√	√	1.573	1.392	0.181	11.51	88.5

TABLE XIV. FAULT DETECTION, CLASSIFICATION AND LOCATION ON IEEE-34 BUS FEEDER AT NODE 802 WITH IBDGs

R_f (Ω)	Fault detection	Fault classification	Node 806 (1.625 km)	Estimated fault location (km)	Absolute error	Relative error (%)	Accuracy (%)
0.1	√	√	1.573	1.540	0.033	2.10	97.9
0.2	√	√	1.573	1.528	0.045	2.86	97.1
0.3	√	√	1.573	1.504	0.069	4.39	95.6
0.4	√	√	1.573	1.500	0.073	4.64	95.4
0.5	√	√	1.573	1.491	0.082	5.21	94.8
0.6	√	√	1.573	1.483	0.090	5.72	94.3
0.7	√	√	1.573	1.470	0.103	6.55	93.5
0.8	√	√	1.573	1.450	0.123	7.82	92.2
0.9	√	√	1.573	1.410	0.163	10.36	89.6
1.0	√	√	1.573	1.383	0.190	12.10	87.9

TABLE XV. FAULT DETECTION, CLASSIFICATION AND LOCATION ON IEEE-34 BUS FEEDER AT NODE 802 WITH SBDGs

R_f (Ω)	Fault detection	Fault classification	Node 806 (1.625 km)	Estimated fault location (km)	Absolute error	Relative error (%)	Accuracy (%)
0.1	√	√	1.573	1.521	0.052	3.31	96.7
0.2	√	√	1.573	1.520	0.053	3.37	96.6
0.3	√	√	1.573	1.498	0.075	4.77	95.2
0.4	√	√	1.573	1.493	0.080	5.09	94.9
0.5	√	√	1.573	1.487	0.086	5.47	94.5
0.6	√	√	1.573	1.474	0.099	6.29	93.7
0.7	√	√	1.573	1.460	0.113	7.18	92.8
0.8	√	√	1.573	1.413	0.160	10.17	89.8
0.9	√	√	1.573	1.381	0.192	12.21	87.8
1.0	√	√	1.573	1.342	0.231	14.69	85.3

TABLE XVI. FAULT DETECTION, CLASSIFICATION AND LOCATION ON IEEE-34 BUS FEEDER AT NODE 802 WITH IBDGS AND SBDGS

R_f (Ω)	Fault detection	Fault classification	Node 806 (1.625 km)	Estimated fault location (km)	Absolute error	Relative error (%)	Accuracy (%)
0.1	√	√	1.573	1.537	0.036	2.29	97.7
0.2	√	√	1.573	1.526	0.047	2.99	97.0
0.3	√	√	1.573	1.502	0.071	4.51	95.5
0.4	√	√	1.573	1.65	0.077	4.90	95.1
0.5	√	√	1.573	1.49	0.083	5.28	94.7
0.6	√	√	1.573	1.478	0.095	6.04	94.0
0.7	√	√	1.573	1.468	0.105	6.68	93.3
0.8	√	√	1.573	1.431	0.142	9.03	91.0
0.9	√	√	1.573	1.76	0.187	11.89	88.1
1.0	√	√	1.573	1.352	0.22	14.05	86.0

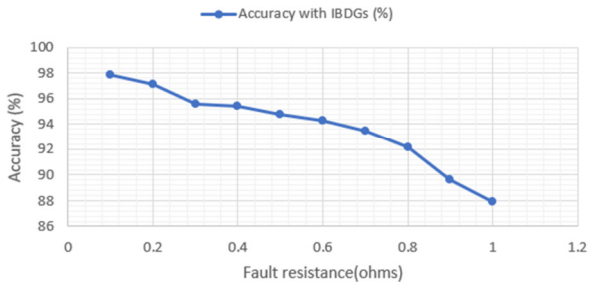

Fig. 19. Fault resistance versus accuracy for all fault types with IBDGs.

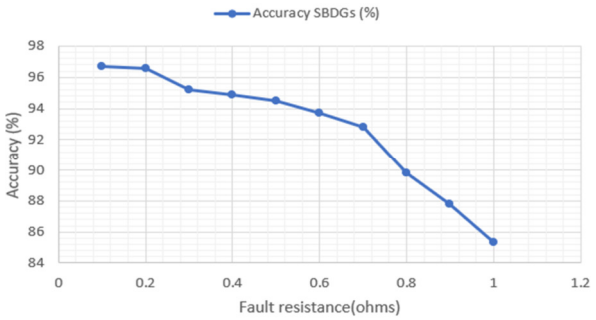

Fig. 20. Fault resistance versus accuracy for all fault types with SBDGs.

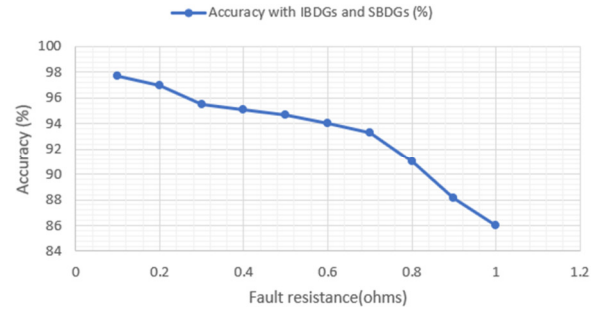

Fig. 21. Fault resistance versus accuracy for all fault types with IBDGs and SBDGs.

The result comparison is shown in Table XVII and Figure 22. It can be seen that the fault location accuracy without DGs is the highest, followed by IBDGs fault location accuracy. The overall result clearly shows that, as the fault resistances of each type of fault increases, the accuracy of the fault location decreases.

TABLE XVII. FAULT DIAGNOSIS COMPARATIVE RESULTS

R_f (Ω)	Accuracy (%)			
	Without DGs	**With IBDGs**	**With SBDGs**	**With IBDGs and SBDGs**
0.1	98.1	97.9	96.7	97.7
0.2	97.3	97.1	96.6	97.0
0.3	96.2	95.6	95.2	95.5
0.4	96.1	95.4	94.9	95.1
0.5	94.9	94.8	94.5	94.7
0.6	94.4	94.3	93.7	94.0
0.7	94.2	93.5	92.8	93.3
0.8	93.3	92.2	89.8	91.0
0.9	89.8	89.0	87.8	88.1
1.0	88.5	87.9	85.3	86.0

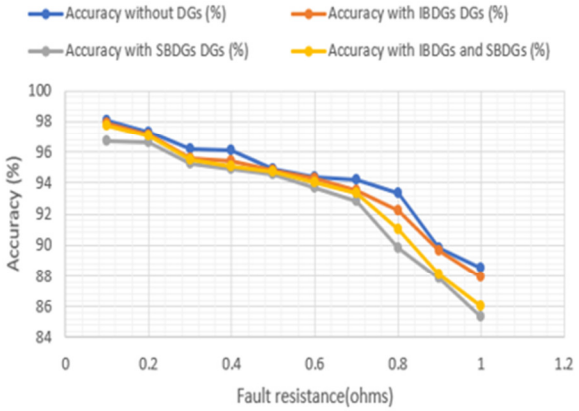

Fig. 22. Accuracy vs fault resistance for fault types without and with DGs.

G. Effect of the DG Type (Upstream and Downstream) on the Fault Location DLANN Method

The IEEE 34 bus network was used to test the above mentioned algorithms in order to look into how distribution networks are affected by DGs. Table XVIII lists the lengths of the lines, each of which has an impedance of 0.01 Ω/km. Assume that the DG unit has been installed at buses 808 and 812 and that there have been isolated instances of single-phase to ground faults between buses 800 and 812 in order to accurately perceive the effect of the unit. As seen in Figure 23, it is upstream (at bus 808) for faults between buses 808 and 812, whereas, in Figure 24, the DG unit is positioned downstream (at bus 812) for faults between buses 800 and 812.

TABLE XVIII. DISTRIBUTION NETWORK LINE LENGTH

Bus	800 - 802	802 - 806	802 - 808	808 - 812	812 - 814
Length (km)	1.573	2.625	20.702	45.134	63.257

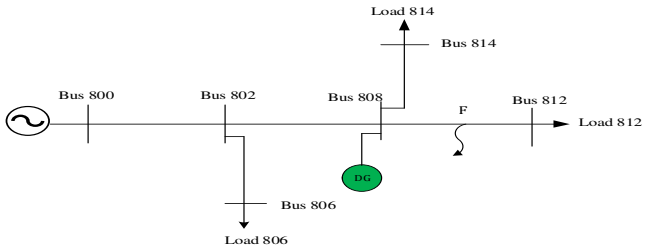

Fig. 23. Distribution network with DG upstream of the fault.

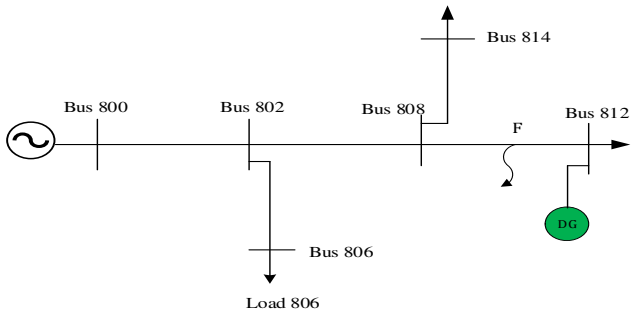

Fig. 24. Distribution network with DG downstream of the fault.

Assume that, in accordance with Figure 23, the DG unit is linked to bus 808 in order to examine the impact of upstream DG on the problem. As previously stated, in this instance, only the zero-sequence component of the DG fault current is significant for computations. Figure 24 shows that the amount of calculation error is lower than in the case of the downstream DG connected to bus 812. The computation error for fault localization with the presence of DG unit considering various fault locations is provided in Tables XIX and XX. It is evident that the presence of a DG unit decreased calculation precision.

TABLE XIX. ERROR WITH IBDGs AND SBDGs UPSTREAM OF FAULT USING ONE END TERMINAL MEASUREMENT

Scenarios		**Fault location from bus 800**			
		Node/Actual distance	Estimated distance (km)	Relative error (%)	Accuracy (%)
Without DG		802 (1.573 km)	1.574	0.06	99.9
		806 (2.625 km)	2.627	0.08	99.9
		808 (22.275 km)	22.32	0.21	99.8
DG upstream of the fault	SBDG	802 (1.573 km)	1.681	0.13	99.87
		806 (2.625 km)	2.735	0.36	99.64
		808 (22.275 km)	23.410	0.61	99.39
	IBDG	802 (1.573 km)	1.662	0.08	99.92
		806 (2.625 km)	2.549	0.30	99.70
		808 (22.275 km)	23.12	0.43	99.57

TABLE XX. ERROR WITH AND WITHOUT IBDGs AND SBDGs DOWNSTREAM OF FAULT USING ONE END TERMINAL MEASUREMENT

Scenarios		**Fault location from bus 800**			
		Node/Actual distance	Estimated distance (km)	Relative error (%)	Accuracy (%)
Without DG		802 (1.573 km)	1.574	0.06	99.9
		806 (2.625 km)	2.627	0.08	99.9
		808 (22.275 km)	22.32	0.21	99.8
DG downstream of the fault	SBDG	802 (1.573 km)	1.681	0.18	99.82
		806 (2.625 km)	2.735	0.53	99.47
		808 (22.275 km)	23.410	0.97	99.03
	IBDG	802 (1.573 km)	1.662	0.16	99.84
		806 (2.625 km)	2.549	0.6	99.40
		808 (22.275 km)	23.12	0.86	99.14

Looking at Figure 25–28, it is evident that the calculation error resulting from the existence of the DG unit is nearly comparable to that of the scenario where it is not present at locations close to the distribution bus. This problem arises because, in this instance, the distribution network injects the majority of the short circuit current. In contrast, because the DG unit is upstream of the fault, there is a significant computation error for the faults between buses 808 and 812. In front of the DG unit, the impedance increases as the problem gets closer to bus 12. As a result, computation error rises. On the other hand, since the DG unit is located upstream of the faults between buses 808 and 812, calculation error originating from the presence of DG is less than the cases in which the DG unit has been placed at downstream. Also, it is clear that the calculation error for the inverter-based DG is less than that for synchronous DG.

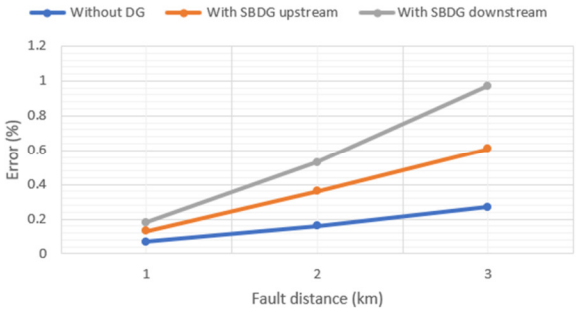

Fig. 25. Computational error with SBDG.

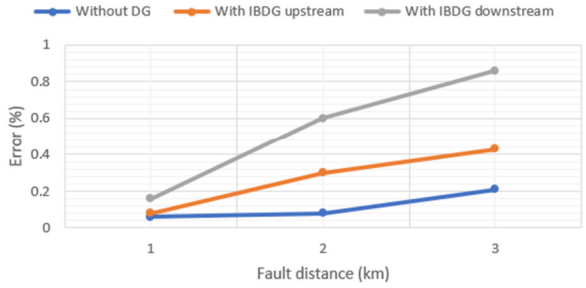

Fig. 26. Computational error with IBDG.

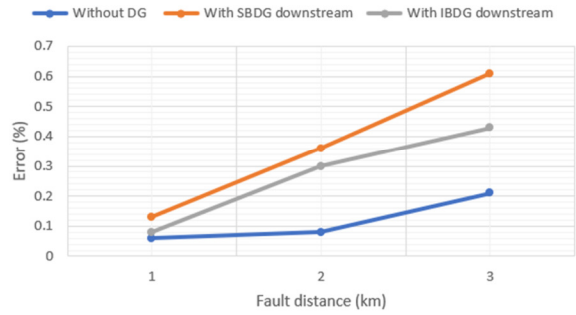

Fig. 27. Computational error with both SBDG and IBDG downstream of the fault.

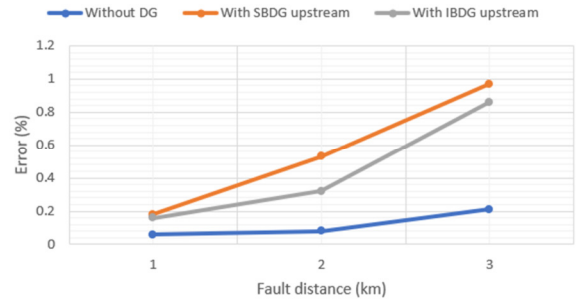

Fig. 28. Computational error with both SBDG and IBDG upastream of the fault.

H. Performance Comparison with Other Methods

In general, fault location methods in distribution systems can be divided into two categories, conventional methods and artificial intelligence methods. The advantages of conventional fault location methods are the simple measurement setup and the less time required for computation. However, their

disadvantages are that they can be inaccurate for large power system networks and when measurement errors are considered. The main advantage of the artificial intelligence fault location methods is that the accuracy is very high even for large power system networks and when measurement errors are considered. Therefore, it is necessary to compare the proposed fault location method to other methods in order to assess its effectiveness and accuracy. All the methods were evaluated using the IEEE 34 bus as a bench mark in real medium and low voltage networks. The result showed that, the proposed method has a higher accuracy or lower average error of 0.1% compared to other techniques (Table XXI) and therefore this method can be used widely by distribution network operators.

TABLE XXI. PERFORMANCE COMPARISON

Ref	Method	Grid (IEEE 34)	Fault types	Error (%)
[31]	SVM	√	All	2.0
[32]	ANN & KNN	√	All	1.2
[33]	ANN	√	All	1.9
Proposed	DLANN	√	All	0.1

IV. CONCLUSION

This paper proposed a DLANN-based algorithm for fault detection, classification and location in a distribution system with intergraded DGs. The paper discussed fault diagnosis without and with IBDGs, SBDGs and both DG types. The simulation results demonstrated that 100% fault detection and classification accuracy was achieved whereas the average fault location accuracy results obtained for no DGs, IBDGs, SBDGs and both DGs was about 99.94%, 99.91%, 99.86% and 99.88% respectively. Fault location accuracy without DGs was the highest (99.4%) because there is no DG influence or contribution to fault current level in the distribution network that could affect it. Fault location accuracy with IBDGs (99.91%) was higher than for SBDGs (99.86%), because the IBDGs do not tolerate high levels of fault current due to the presence of power electronic devices compared to SBDGs. The average fault location accuracy for the case of combining IBDGs and SBDGs was 99.88% and was midway between IBDGs and SBDGs. The overall results showed that the fault location accuracy without DGs (99.4%) is better than those with DGs whether being IBDGs or SBDGs, because the DG fault current contribution to the distribution network reduces fault location accuracy. The effects of fault resistance and fault distance were also examined. It was discovered that the accuracy of fault location falls as fault resistance increases and vice versa. The effect of fault distance revealed that the accuracy of fault location decreased as the fault point was moved farther away from the substation and increased when the fault occurred closer to the substation. Analysis of the type of DGs (upstream or downstream) on the IEEE 34 bus test system on fault locating techniques was also conducted. It was found that the functioning of fault locating techniques can be impacted by the DG units' involvement in fault currents. Research indicates that fault locating techniques benefit more from upstream than from downstream DGs. The impact of two different kinds of DGs on the placement of faults was examined. Inverter-based DGs inject less short-circuit current to the fault, so, their efficacy surpasses that of synchronous DGs. To maintain the safety and dependable operation of the power system, the research findings and methods can be used to enhance the distribution system's protective scheme as DG penetration rises.

ACKNOWLEDGMENT

The authors are grateful to the Pan African University Institute for Basic Sciences, Technology and Innovation (PAUSTI) for the support.

REFERENCES

[1] S. S. Gururajapathy, H. Mokhlis, and H. A. Illias, "Fault location and detection techniques in power distribution systems with distributed generation: A review," *Renewable and Sustainable Energy Reviews*, vol. 74, pp. 949–958, Jul. 2017, https://doi.org/10.1016/j.rser.2017.03.021.

[2] M. Shafiullah and M. A. Abido, "A Review on Distribution Grid Fault Location Techniques," *Electric Power Components and Systems*, vol. 45, no. 8, pp. 807–824, May 2017, https://doi.org/10.1080/15325008.2017.1310772.

[3] S. Shi, B. Zhu, A. Lei, and X. Dong, "Fault Location for Radial Distribution Network via Topology and Reclosure-Generating Traveling Waves," *IEEE Transactions on Smart Grid*, vol. 10, no. 6, pp. 6404–6413, Aug. 2019, https://doi.org/10.1109/TSG.2019.2904210.

[4] A. Tashakkori, P. J. Wolfs, S. Islam, and A. Abu-Siada, "Fault Location on Radial Distribution Networks via Distributed Synchronized Traveling Wave Detectors," *IEEE Transactions on Power Delivery*, vol. 35, no. 3, pp. 1553–1562, Jun. 2020, https://doi.org/10.1109/TPWRD.2019.2948174.

[5] H. Cifuentes-Chaves, J. Mora-Florez, and S. Perez-Londono, "Time domain analysis for fault location in power distribution systems considering the load dynamics," *Electric Power Systems Research*, vol. 146, pp. 331–340, May 2017, https://doi.org/10.1016/j.epsr.2017.01.034.

[6] R. Dashti, M. Daisy, H. R. Shaker, and M. Tahavori, "Impedance-Based Fault Location Method for Four-Wire Power Distribution Networks," *IEEE Access*, vol. 6, pp. 1342–1349, Jan. 2018, https://doi.org/10.1109/ACCESS.2017.2778427.

[7] Y. V. Tresso, R. A. S. Fernandes, and D. V. Coury, "Reducing multiple estimation for fault location in medium voltage distribution networks," *Electric Power Systems Research*, vol. 199, Oct. 2021, Art. no. 107424, https://doi.org/10.1016/j.epsr.2021.107424.

[8] F. C. L. Trindade and W. Freitas, "Low Voltage Zones to Support Fault Location in Distribution Systems With Smart Meters," *IEEE Transactions on Smart Grid*, vol. 8, no. 6, pp. 2765–2774, Aug. 2017, https://doi.org/10.1109/TSG.2016.2538268.

[9] R. F. Buzo, H. M. Barradas, and F. B. Leao, "A New Method for Fault Location in Distribution Networks Based on Voltage Sag Measurements," *IEEE Transactions on Power Delivery*, vol. 36, no. 2, pp. 651–662, Apr. 2021, https://doi.org/10.1109/TPWRD.2020.2987892.

[10] J. Zhang, Z. Y. He, S. Lin, Y. B. Zhang, and Q. Q. Qian, "An ANFIS-based fault classification approach in power distribution system," *International Journal of Electrical Power & Energy Systems*, vol. 49, pp. 243–252, Jul. 2013, https://doi.org/10.1016/j.ijepes.2012.12.005.

[11] M. Khodayar, G. Liu, J. Wang, and M. E. Khodayar, "Deep learning in power systems research: A review," *CSEE Journal of Power and Energy Systems*, vol. 7, no. 2, pp. 209–220, Mar. 2021, https://doi.org/10.17775/CSEEJPES.2020.02700.

[12] J. Xie, G. Du, C. Shen, N. Chen, L. Chen, and Z. Zhu, "An End-to-End Model Based on Improved Adaptive Deep Belief Network and Its Application to Bearing Fault Diagnosis," *IEEE Access*, vol. 6, pp. 63584–63596, Jan. 2018, https://doi.org/10.1109/ACCESS.2018.2877447.

[13] W. Mao, W. Feng, Y. Liu, D. Zhang, and X. Liang, "A new deep auto-encoder method with fusing discriminant information for bearing fault diagnosis," *Mechanical Systems and Signal Processing*, vol. 150, Mar. 2021, Art. no. 107233, https://doi.org/10.1016/j.ymssp.2020.107233.

[14] Y.-C. Huang and P.-J. Wang, "Infrared Air Turbine Dental Handpiece Rotor Fault Diagnosis with Convolutional Neural Network," *Sensors and Materials*, vol. 32, no. 11, pp. 3545–3558, Nov. 2020, https://doi.org/10.18494/sam.2020.2755.

[15] Q. Wu, K. Ding, and B. Huang, "Approach for fault prognosis using recurrent neural network," *Journal of Intelligent Manufacturing*, vol. 31, no. 7, pp. 1621–1633, Oct. 2020, https://doi.org/10.1007/s10845-018-1428-5.

[16] I. Goodfellow *et al.*, "Generative Adversarial Nets," in *Advances in Neural Information Processing Systems*, 2014, vol. 27.

[17] X. Tang, Z. Xu, and Z. Wang, "A Novel Fault Diagnosis Method of Rolling Bearing Based on Integrated Vision Transformer Model," *Sensors*, vol. 22, no. 10, Jan. 2022, Art. no. 3878, https://doi.org/10.3390/s22103878.

[18] T. Li, Z. Zhao, C. Sun, R. Yan, and X. Chen, "Multireceptive Field Graph Convolutional Networks for Machine Fault Diagnosis," *IEEE Transactions on Industrial Electronics*, vol. 68, no. 12, pp. 12739–12749, Sep. 2021, https://doi.org/10.1109/TIE.2020.3040669.

[19] M. W. Akram *et al.*, "CNN based automatic detection of photovoltaic cell defects in electroluminescence images," *Energy*, vol. 189, Dec. 2019, Art. no. 116319, https://doi.org/10.1016/j.energy.2019.116319.

[20] C.-F. Jeffrey Kuo, S.-H. Chen, and C.-Y. Huang, "Automatic detection, classification and localization of defects in large photovoltaic plants using unmanned aerial vehicles (UAV) based infrared (IR) and RGB imaging," *Energy Conversion and Management*, vol. 276, Jan. 2023, Art. no. 116495, https://doi.org/10.1016/j.enconman.2022.116495.

[21] A. Yılmaz and G. Bayrak, "A real-time UWT-based intelligent fault detection method for PV-based microgrids," *Electric Power Systems Research*, vol. 177, Dec. 2019, Art. no. 105984, https://doi.org/10.1016/j.epsr.2019.105984.

[22] I. A. Shah, I. U. Khalil, M. I. A. Shah, N. Mohamed, E. Ali, and S. S. M. Ghoneim, "MI2T-UNet: Integrating Multi-Scale Input Image and Top-hat Context for Infrared Small Object Segmentation." Research Square, Jul. 24, 2023, https://doi.org/10.21203/rs.3.rs-3164396/v1.

[23] "Data Preprocessing - an overview | ScienceDirect Topics." https://www.sciencedirect.com/topics/engineering/data-preprocessing.

[24] L. Alzubaidi *et al.*, "Review of deep learning: concepts, CNN architectures, challenges, applications, future directions," *Journal of Big Data*, vol. 8, no. 1, Mar. 2021, Art. no. 53, https://doi.org/10.1186/s40537-021-00444-8.

[25] M. M. Taye, "Understanding of Machine Learning with Deep Learning: Architectures, Workflow, Applications and Future Directions," *Computers*, vol. 12, no. 5, May 2023, Art. no. 91, https://doi.org/10.3390/computers12050091.

[26] I. H. Sarker, "Deep Learning: A Comprehensive Overview on Techniques, Taxonomy, Applications and Research Directions," *SN Computer Science*, vol. 2, no. 6, Aug. 2021, Art. no. 420, https://doi.org/10.1007/s42979-021-00815-1.

[27] J. Heaton, *Introduction to Neural Networks with Java*, 2nd Edition. Chesterfield, MO, USA: Heaton Research, 2008.

[28] S. F. Alwash, V. K. Ramachandaramurthy, and N. Mithulananthan, "Fault-Location Scheme for Power Distribution System with Distributed Generation," *IEEE Transactions on Power Delivery*, vol. 30, no. 3, pp. 1187–1195, Jun. 2015, https://doi.org/10.1109/TPWRD.2014.2372045.

[29] H. Saadat, *Power system analysis*. New Delhi, India: Mc Graw-Hill, 2006.

[30] R. A. Walling, R. Saint, R. C. Dugan, J. Burke, and L. A. Kojovic, "Summary of Distributed Resources Impact on Power Delivery Systems," *IEEE Transactions on Power Delivery*, vol. 23, no. 3, pp. 1636–1644, Jul. 2008, https://doi.org/10.1109/TPWRD.2007.909115.

[31] R. Perez, C. Vasquez, and A. Viloria, "An intelligent strategy for faults location in distribution networks with distributed generation," *Journal of Intelligent & Fuzzy Systems*, vol. 36, no. 2, pp. 1627–1637, Jan. 2019, https://doi.org/10.3233/JIFS-18807.

[32] S. Jamali, A. Bahmanyar, and S. Ranjbar, "Hybrid Classifier for Fault Location in Active Distribution Networks," *Protection and Control of Modern Power Systems*, vol. 5, no. 2, pp. 1–9, Apr. 2020, https://doi.org/10.1186/s41601-020-00162-y.

[33] F. Dehghani, F. Khodnia, and E. Dehghan, "Fault location of unbalanced power distribution feeder with distributed generation using neural networks," *CIRED*, vol. 2017, no. 1, pp. 1134–1137, Oct. 2017, https://doi.org/10.1049/oap-cired.2017.0007.